

A sea-level rise curve from Guilford, Connecticut, USA

Koren R. Nydick, Alison B. Bidwell, Ellen Thomas¹, Johan C. Varekamp

Department of Earth and Environmental Sciences, Wesleyan University, Middletown, CT 06459, USA

Received 13 April 1994; revision accepted 21 September 1994

Abstract

High-resolution stratigraphic studies based on sediment chemistry, lithology, macroflora, and benthic foraminiferal assemblages in three peat cores from coastal salt marshes at Guilford, Connecticut, show that coastal marshes are ephemeral environments. Marsh-wide environmental variations were common, and century-long episodes of relative submergence alternated with emergence. Despite about 2 m of relative sea-level rise (RSLR) in Connecticut over the last 1500 years, the marshes have expanded both landwards and seawards, and marsh accretion has been outpaced only marginally by RSLR.

We used radiocarbon dating and the level of anthropogenic markers (metal pollution, as dated with ²¹⁰Pb) in the cores for age control. For most of the last 1000 years the rate of RSLR was between 1.3 and 1.8 mm/yr, but over the last 300–400 years it increased to 2.9–3.3 mm/yr, and has been faster than the accretion rate, especially in the middle marsh. The net-submergence rate or “submergence index” (ratio of the rate of RSLR and marsh-accretion rate) averaged about 1.15 over the last 1000 years, and increased to about 1.5 over the last 200 years.

The rate of RSLR was very sluggish during the early part of the Little Ice Age, but we found a slightly higher rate during the Little Climate Optimum; this excursion is close to the noise level, however. The most significant observation is that RSLR increased strongly around A.D. 1650. The onset of this acceleration falls in the middle to end of the Little Ice Age, and thus preceded the period of modern global warming that started late last century and that has been tentatively correlated with anthropogenic emissions of greenhouse gases.

1. Introduction

1.1. Climate and sea-level rise

Global sea level has been rising for more than ten thousand years, leading to the establishment and expansion of coastal salt marshes (e.g., Redfield and Rubin, 1962; Redfield, 1967, 1972; Lambeck, 1990). Stratigraphic studies of peat deposits in salt marshes provide insight into the rates of relative sea-level rise (RSLR) at different time scales (e.g., Niering et al., 1977; Rampino,

1979; Van de Plassche et al., 1989; Van de Plassche, 1991; Scott and Medioli, 1978, 1986; Scott et al., 1986, 1987; Allen, 1990a, 1991; French et al., 1990; Fletcher et al., 1993a,b). The average rate of RSLR in New England from 7000 to 3000 yrs B.P. was about 3 mm/yr, with a possible high stand around 4000 yrs B.P. (Scott et al., 1986, 1987; Gayes et al., 1992), which is not recognized in all sea-level rise curves (e.g., Belknap and Kraft, 1977; Fletcher et al., 1993b). About 3000 yr ago RSLR decelerated to less than 1 mm/yr (Bloom and Stuiver, 1963; Peltier and Tushingham, 1991; Tooley, 1993; Patton and Horne, 1992). This deceleration may be related to true changes in the eustatic rate, or changes in the rate of crustal movements (Warrick, 1993; Woodworth, 1993).

¹ Also at: Center for the Study of Global Change, Yale University, New Haven, CT 06520, USA.

This deceleration was not synchronous with documented changes in climate, but might have been a delayed effect of the termination of the Holocene hypsithermal (4000–5000 yrs B.P.; Lamb, 1977; Wigley, 1990; Anderson, 1991).

Local RSLR records reflect, in addition to global changes in sea level, the local rate of crustal rebound after the last glacial period, tectonic activity, and redistribution of water masses in the oceans due to changes in global climate (e.g., Roemmich, 1992; Varekamp et al., 1992; Fletcher, 1993b; Mörrner, 1993). Distillation of global sea-level rise patterns from a collection of local records is therefore complex (e.g., Scott et al., 1987; Gornitz, 1992; Douglas, 1991, 1992; Groeger and Plag, 1993; Warrick, 1993).

Estimates of potential future changes in sea level related to predicted global warming as a result of the increased concentrations of greenhouse gases in the atmosphere (e.g., Houghton et al., 1990,

1992; Wigley and Raper, 1992, 1993) carry large uncertainties. To better understand potential future changes in the rate of RSLR, we tried to resolve rate changes in RSLR over the last few thousand years on a centennial time scale or better. Indications for strong variations in the rate of RSLR over the last 1500 years were found in marshes near Clinton, CT (Thomas and Varekamp, 1991; Van de Plassche, 1991; Varekamp et al., 1992). We present data from the Guilford marshes, located about 15 km west of Clinton in Connecticut along Long Island Sound (Fig. 1).

1.2. Estimating rate changes in relative sea-level rise

Studies of peat sequences have documented an overall rise in sea level over the last ten millennia (e.g., Bloom and Stuiver, 1963; Rampino, 1979; Van de Plassche et al., 1989; Allen, 1990a,b, 1991),

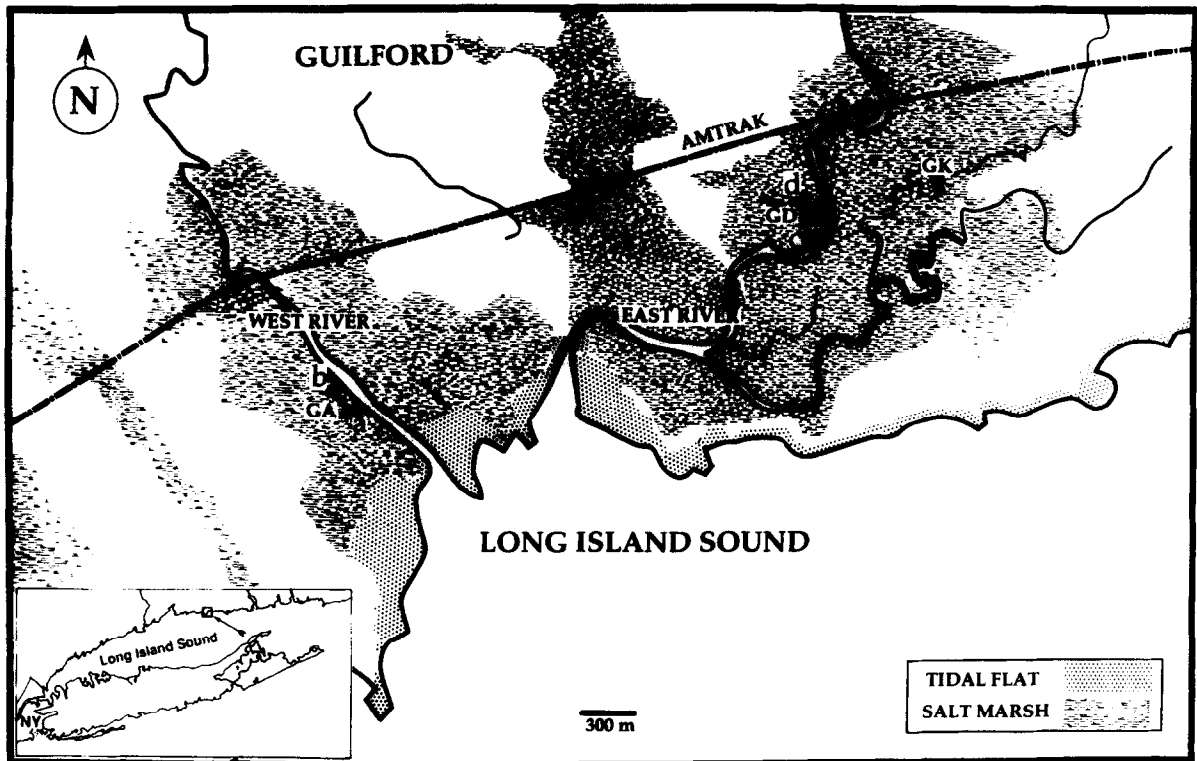


Fig. 1. The Guilford marshes in Connecticut along the West River and East River. Locations of core sites and transects *a-b* and *d-c* for Fig. 3 are indicated.

but high-resolution studies of the rates of RSLR in marsh sequences are hampered by many factors. These include artifacts of sampling (e.g., compaction, stretching; Bloom, 1964; Harrison and Bloom, 1977; Allen, 1990a), and problems with age dating because of the imprecision in ^{14}C dating and complexities in using ^{210}Pb dating (e.g., Turekian et al., 1980; Varekamp, 1991). In addition, salt marshes occupy a substantial vertical range depending upon tidal range; along Long Island Sound about 0.5–1.2 m. The reconstruction of RSLR from age–depth graphs based on data from peat samples without constraints on their paleo-distance from sea level thus carries large uncertainties.

The paleo-position of a peat sample within the intertidal zone can potentially be determined by comparing core samples to samples from the modern marsh, which is zoned from sea to land. Marshes are zoned in macroflora (Redfield and Rubin, 1962; Redfield, 1972; Niering et al., 1977; Nixon, 1982; Orson et al., 1987; Bertness, 1992), in microfauna (Scott and Medioli, 1980, 1986; Scott and Leckie, 1990), in sediment chemistry (Allen, 1987; Allen and Rae, 1988; Varekamp et al., 1992) and in lithology (Thomson et al., 1975; McCaffrey and Thomson, 1980; French et al., 1990), all parameters reflecting the changes in inundation frequency. The zones occur at well-defined vertical ranges from sea level, as shown by these studies in modern marshes. Recent marsh zonations may not always reflect paleo-environments truthfully, however, because of extensive ditching since the 1920s. In addition, the exact dependency of the marsh zonation on tidal parameters has not yet been investigated in detail (Varekamp and Thomas, unpub. data).

Marsh accretion rates differ between the marsh zones, with commonly higher accretion rates in the low marsh. High accretion rates, predominantly of macrophytic remains, are also found in the *Phragmites* brackish/fresh-water marsh fringes (Allen, 1990a,b,c; French et al., 1990; French and Spencer, 1993). When the rate of RSLR changes, a marsh will either submerge or emerge, and the depositional environment will shift until the local accretion rate matches the rate of RSLR (Varekamp et al., 1992; French et al., 1990; Allen,

1990a,c, 1992, 1994; Varekamp and Thomas, work in progress). Relative submergences and emergences of a marsh have been labeled “sea-level rise tendencies” (Shennan, 1986a,b), or ROB and TOBs (regressive and transgressive overlap boundaries; Tooley, 1982; Van de Plassche, 1991; Fletcher et al., 1993b).

We used as paleoenvironmental proxies the abundances and types of macrofloral remains (stems, roots, rhizomes, and leaves), the relative abundances of agglutinated benthic foraminifera and thecamoebians, iron and sulfur abundances, and weight loss-on-ignition (LOI) data, the latter as an estimate for the ratio clay/organic matter, and the $\delta^{13}\text{C}$ value of the samples used for ^{14}C -dating. *Spartina* species are common in middle and low marsh, and are C-4 plants, with $\delta^{13}\text{C}$ values between -10 and -13‰ , whereas *Phragmites* species, occurring along the fresh-water fringes of the marshes, follow the C-3 pathway in photosynthesis, and have $\delta^{13}\text{C}$ values between -20 and -25‰ (Ember et al., 1987).

The sulfur content of coastal peats depends on the limiting parameter of sulfide fixation after deposition. The iron content is limiting to sulfur fixation in organic-rich peats (Berner, 1984, 1985; Canfield, 1989; Varekamp, 1991), whereas the organic carbon content may be limiting in clay-rich sediments (Giblin, 1988). The highest marsh environments are flooded by sea water twice a month only, and sulfate availability may limit the rate of sulfur fixation and thus the sulfur concentration in these sediments. Because the sulfur abundance represents post-depositional (diagenetic) processes, it can only be used as an indirect proxy for changes in flooding frequency. Sulfur diffuses into the sediment column where it is gradually fixed by soluble iron into pyrite, and the top 10 to 15 cm of the cores commonly have low sulfur levels because the diagenetic process is ongoing (Varekamp, 1991; Varekamp et al., 1992). The iron contents are a proxy for the presence of fine-grained sediment (Varekamp, 1991).

The foraminiferal data provided the most sensitive parameter of marsh zonation, because the foraminifera live on the marsh surface or in the topmost, oxygenated few millimeters of the sediment. They are buried in an environment with

limited or no bioturbation, because the sediments are anoxic except for the top few millimeters, and the dense root-mat system in the high and middle marsh prevents bioturbation by larger invertebrates. We used the zonal relations derived by Scott and Medioli (1980) to derive the position of the paleo-marsh surface with respect to mean high water (MHW) during deposition, after recalibration to the local tidal frame and comparison to data on surface samples from the modern marsh. Using this method, we reconstructed paleo-depositional environments with an approximate precision of ± 15 cm from paleo-MHW. We converted the raw data to rates of RSLR through dating of the sequence, and subsequently to MHW-rise curves (Thomas and Varekamp, 1991; Varekamp et al., 1992). We obtained all data from the same coring site and thus obtain a continuous record if the sedimentation at the site was continuous. The age is interpolated between age markers, with minor adjustments for changes in accretion rate by depositional facies.

2. Study sites and methods

The Guilford marshes, along the East and West River (Fig. 1), grade from low marsh near the coast to extensive high and middle marsh with *Spartina patens* meadows further upstream. A narrow rim of *Phragmites* stands occurs on the landward side in many places. The modern marsh environment has been modified by the excavation of a marina, and ditching for mosquito control. Wooded “islands” of hard rock and glacial deposits have remained emerged during the time of salt marsh growth. The local tidal range (1.65 m), highest astronomical tide and average high water at spring tides were derived from NOAA tide tables (NOS, 1992).

Field studies of the two marsh lobes established a general lithological stratigraphic framework, based on 70 cores of about 2 m length (Nydick, 1993), and three cores were selected for detailed studies (Fig. 1). Cores were taken with a lacquer-coated, cast-iron 1.5 m long, open-barrel corer with a diameter of about 15 cm, which provides undisturbed, uncompacted continuous cores.

Cores were wrapped airtight, and carried in aluminum core holders to the laboratory where they were described, photographed and sampled continuously. Cores were sliced into 40 to 50 samples (2–5 cm slice thickness), which were analyzed for all proxy parameters. Upon arrival in the laboratory, samples for foraminiferal studies were directly processed (Scott and Medioli, 1980, 1986; Thomas and Varekamp, 1991; Appendices 1–3).

The sediment chemistry was determined on the $< 180 \mu\text{m}$ fraction. In one set of experiments, the air-dried screened sediments were leached for 8 hours in an orbital shaker with an acid/oxidizing $\text{HCl-HNO}_3\text{-H}_2\text{O}_2$ solution. The leachates were filtered, brought up to volume, diluted and analyzed for Fe, Zn and Cu with an Atomic Absorption Spectrometer (Perkin Elmer 372). Another aliquot was neutralized with NaOH, and SO_4 contents were determined by Ion Chromatography (Dionex QIC). The sediment samples were heated at 850°C for one hour to obtain maximum Loss-on-Ignition (LOI) data (Varekamp, 1991). These LOI data provide approximate contents of organic carbon, although in clay-rich samples the devolatilization of clays and roasting of sulfides may contribute several % weight loss. Variations in LOI values that are $< 10\%$ can not be easily interpreted in terms of variations in organic carbon contents.

Age control was obtained by ^{14}C dating; radio-carbon ages were corrected for natural isotope fractionation and calibrated according to Stuiver and Pearson (1993). We determined the level of onset of heavy metal pollution in the three cores, which was dated at Guilford’s West River marsh through extrapolation of ^{210}Pb dates at 1877 ± 15 A.D. (Green, 1988). About five ^{14}C age points per core were established for a total of 17 determinations (Table 1). Plant fragments of only one species were hand-picked from the samples for ^{14}C dating. Up to 15 grams of dry plant material was hand-picked to reduce the counting errors during analyses.

From the benthic foraminiferal data we used the parameter “% other species” (100–% *Trochammina macrescens*) to illustrate overall submergence and emergence trends in the cores (Thomas and Varekamp, 1991); high values of

Table 1
Radiocarbon ages of samples from Guilford marsh sequences

Sample code	Sample interval (cm)	Marsh surface depth (cm ^a)	Plant species	$\delta^{13}\text{C}$ ‰	Isotop. fract. corr. age (yr B.P.)	Calibr. age (yr A.D.)	2 σ range
GA-3	67–73	62	<i>S. alt.</i>	−12.0 ^b	100 ± 70	1716 ^c	(1680–1753)
GA-4	87–90	88	<i>S. pat.</i>	−10.0	370 ± 60	1488	(1432–1657)
GA-2	106–110	103	<i>S. alt.</i>	−13.8	590 ± 60	1398	(1290–1439)
GA-1	119–134	127	wood	−25.0 ^b	720 ± 90	1288	(1165–1411)
GA-5	173–185	173	<i>S. alt.</i>	−14.5	1170 ± 50	886	(726–990)
GD-1	52–55	53	<i>S. pat.</i>	−10.0 ^b	90 ± 70	1714 ^c	(1663–1745)
GD-2	55–60	55	<i>S. alt.</i>	−13.8	10 ± 60	1710 ^c	(1695–1726)
GD-3	55–60	57	<i>S. pat.</i>	−10.0	160 ± 60	1770 ^c	(1647–1889)
GD-4	77–80	79	<i>S. alt.</i>	−10.0	440 ± 60	1446 ^c	(1405–1530)
GD-5	95–100	95	<i>S. alt.</i>	−13.8	600 ± 80	1360 ^c	(1278–1447)
GD-6	136–140	138	<i>S. pat.</i>	−10.0	1070 ± 80	989	(785–1162)
GK-1	66–73	70	<i>S. alt.</i>	−13.2	210 ± 60	1669 ^c	(1525–1793)
GK-2	93–103	98	<i>S. alt.</i>	−10.8	660 ± 70	1302	(1248–1422)
GK-3	115–120	118	<i>S. pat.</i>	−9.7	1020 ± 80	1017	(883–1215)
GK-4	180–185	180	<i>S. alt.</i>	−13.8	1720 ± 70	341	(139–532)
GK-5	180–181	180	<i>S. pat.</i>	−10.0 ^b	1780 ± 70	249	(83–420)
GK-6	186–198	190	mixed	−14.3	1220 ± 80	800	(660–1000)

^a The depth of the paleommarsh surface (in centimeters below the modern marsh surface) was taken 5 cm above major rhizome levels or was taken as the middle of a sample slice in case of pure *S. patens* or pure *S. alterniflora* or was taken as the shallowest point of penetration of *S. alterniflora* roots in a *S. patens* matrix.

^b Assumed $\delta^{13}\text{C}$ based on plant type.

^c Selection of the calibrated ages or 2 σ range, taking the stratigraphic position (depth) into account.

this parameter indicate submergence, low values emergence. To obtain more detailed information from the faunal data, we assigned all samples to faunal subzones according to Scott and Medioli (1980) in order to derive their distances from paleo-MHW, and the level within each zone was estimated based on the total species composition (Fig. 2). The tidal range at Guilford (1.65 m) is greater than that at the Nova Scotia marshes studied by Scott and Medioli (1980) and the Clinton marshes (Thomas and Varekamp, 1991; 1.65 m vs. 1.10 m). The Guilford foraminiferal subzones were adjusted to the greater tidal range according to Scott and Medioli's (1980) statement that the upper zones change little in thickness, and that the larger tidal range is accommodated in lower subzone IIB (Fig. 2).

The distance from paleo-MHW for each sample was plotted in marsh paleo-environment curves (MPE curves; Thomas and Varekamp, 1991). The distances from MHW were subsequently added to

or subtracted from depth-in-core, which provided a curve of paleo-MHW-below-datum versus depth-in-core. The age data for each core were plotted in age–depth graphs and then combined with the last curve to provide a paleo-MHW versus age curve for each core. This curve then is converted to “the level of paleo-MHW below modern MHW” (MMHW) versus age, which is a mean high-water rise curve (MHW curve; see Varekamp et al., 1992, for details); with this technique secular changes in the tidal amplitude will be recorded as RSLR rate changes.

3. Results

3.1. Field data

From bottom to top we distinguish five lithostratigraphical units (Fig. 3), based on logs of about 70 cores: (1) a clay-rich section with

	Floral Zones	Microfaunal Subzones	
		No forams	No forams
HHW - 112.5	High Marsh	IA	<i>T. macrescens</i> *
107.5		IB	<i>T. macrescens</i> * <i>T. comprimata</i> <i>H. manilaensis</i> rare <i>T. inflata</i>
MHWS - 92.5	Middle Marsh	IIA	<i>T. comprimata</i> <i>T. inflata</i> <i>A. mexicana</i> <i>M. fusca</i> rare <i>T. macrescens</i>
MHW - 82.5	Low Marsh A		
MHWN - 67.5	Low Marsh B	IIB	<i>M. fusca</i> <i>A. mexicana</i> <i>T. inflata</i> rare <i>T. comprimata</i> (<i>A. inepta</i>) calcareous species
MSL - 0			
-10			

*possibly thecamoebians and *P. ipohalina*

Fig. 2. Marsh subenvironments with vertical distances from mean sea level (MSL) and foraminiferal assemblages (after Scott and Medioli, 1980; adapted to the Guilford marsh tidal range by Nydick, 1993). HHW: highest high water; MHWS: mean high water at spring tide; MHW: mean high water; MHWN: mean high water at neap tide; MSL: mean sea level.

common *S. alterniflora* roots (E); (2) a black, mushy peat layer with *S. patens*, *Distichlis spicata* and minor *S. alterniflora* remains (D); (3) a red-brown, high-marsh peat layer dominated by *S. patens* and *D. spicata* remains (C); (4) a dark, clay-bearing peat with *S. patens* and *S. alterniflora* remains (AB and B); and (5) the modern peat zone with intact plant roots, particularly of *S. patens* and *D. spicata* (A). The GA core (sea proximal) shows in general more clay-rich depositional environments than the more landward cores.

3.2. Faunal data

The samples show strong variations in faunal assemblages (Fig. 4). The paleo-environments as indicated by faunas through correlation to the subzones as defined in Fig. 2 range from highest marsh (subzone IB/IA) through the boundary of

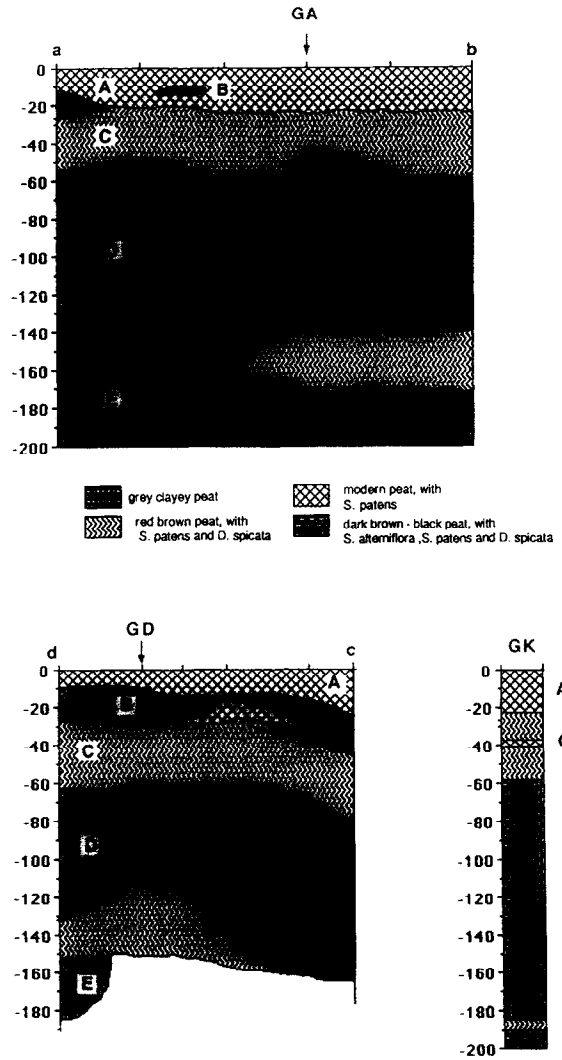


Fig. 3. Lithological profiles along transect a-b, with location of core GA, transect c-d, with location of core GD and the stratigraphy at the GK coring location. Distance a-b is about 300 m, distance c-d about 250 m. All vertical distances are in cm below the modern marsh surface.

subzone IIA/IIB (low marsh). The present marsh surface is in subzone IIA for all three core sites, with GA in its middle, GD lower, and GK high in this subzone. Differences in height between sites GK-GD and GD-GA are 12 cm and 5 cm, respectively, according to faunal assemblages; levelling measurements yielded 10 cm and 5 cm respectively. Core GK shows the largest variation in subzones, with samples representing the highest subzone IB

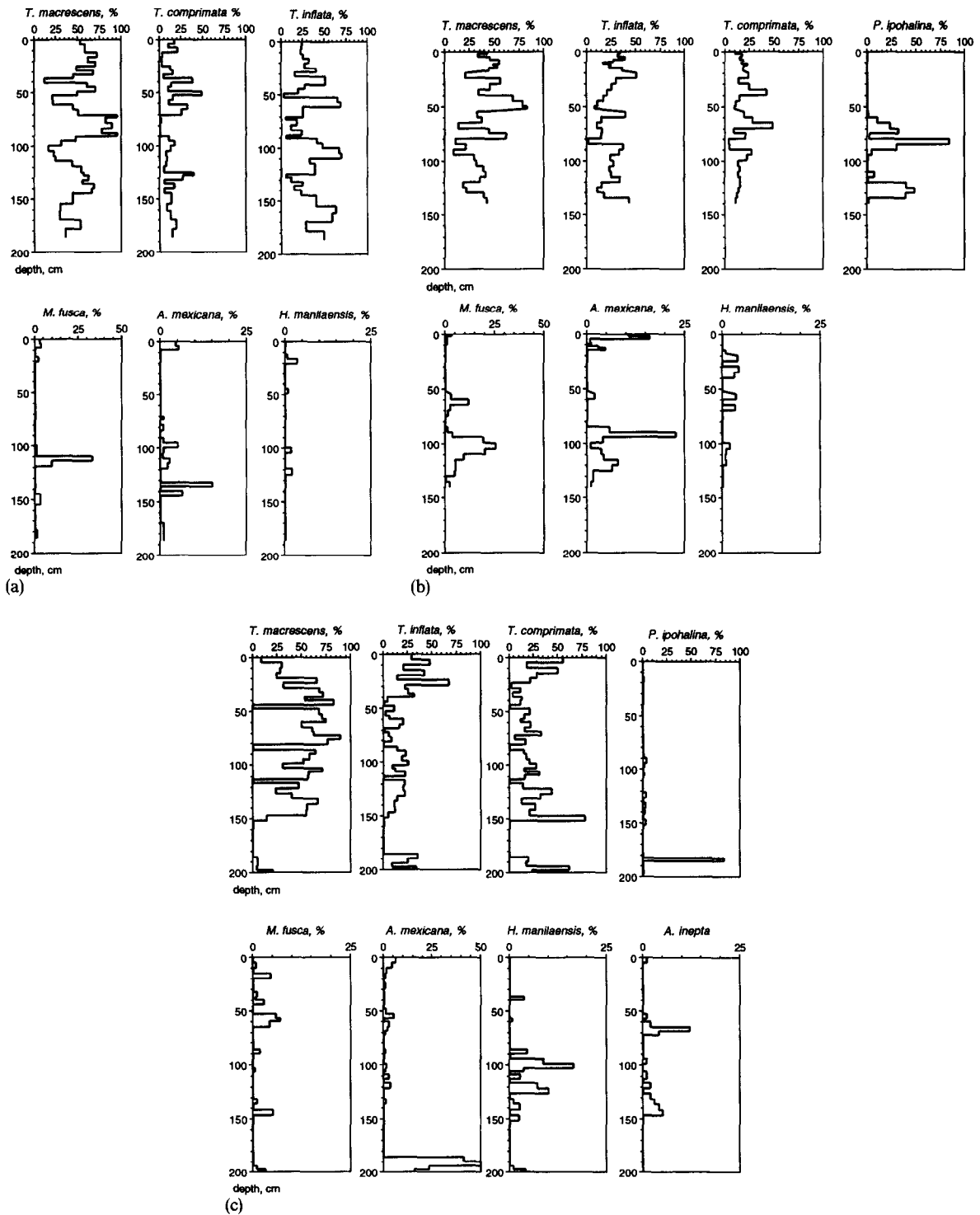


Fig. 4. Relative abundances of the most common foraminiferal species (a: core GA; b: core GD; c: core GK).

(highest marsh) and other samples close to the IIA/IIB boundary (low marsh).

The most common species in the marshes at Guilford as well as in those at Clinton (Thomas and Varekamp, 1991) are the typical middle- to high-marsh species *Trochammina macrescens*, *Trochammina inflata* and *Tiphotrocha comprimata*. *Arenoparrella mexicana* and *Miliammina fusca* occur in some intervals at all three core sites (Appendices 1–3). *Ammoastuta inepta* is present in core GK only; this species is reported from low-marsh settings with low salinities, e.g., in the Mississippi delta (Scott et al., 1991). *Haplophragmoides manilaensis*, an inner estuarine, low-salinity species (Scott and Medioli, 1980; Thomas and Varekamp, 1991) occurs rarely at all three sites. The low salinity species *Pseudothurammina ipohalina* (Scott and Medioli, 1980, 1986) occurs abundantly in a few intervals in cores GK and GD.

The data were plotted in Marsh Paleo-Environmental (MPE) curves (Fig. 5), showing intervals of relative submergence or emergence. We observed a similar alternation of subenvironments in all three cores, labeled L for low marsh and H for high marsh. All cores show submergence around 100 cm depth (L2; in cores GK and GA from 115 to 90 cm), but much less pronounced in core GD (105–95 cm). This was followed by an emergence (H1), represented in a thinner interval

in core GD (80–70 cm) than in cores GA (95–70 cm) and GK (86–70 cm). This emergence was followed by a submergence (L1 at 75–55 cm), which was most pronounced in cores GK and GD. The following emergence (H₀ at 60–50 cm) was also more pronounced at GK and GD, and responsible for the formation of the “red-brown peat layer B” (Fig. 3). The modern period of submergence (MS) occurred from about 50 cm to the marsh surface at core GK, from about 30 cm to the marsh surface at GD, and over the topmost 15 cm at core GA.

In conclusion, cores from the Guilford marshes show overall a slight emergence over the last two meters: from mudflat at about 2 m depth to middle/high marsh in modern times, with depositional environments ranging from highest marsh to middle marsh close to MHW. Over this whole period the marsh growth has thus kept up with, and even slightly outpaced the rate of RSLR, but on shorter time scales the rate of marsh accretion and RSLR were not in equilibrium. The most landward areas of the marsh were most sensitive to changes, whereas the deeper marsh sections show lesser fluctuations in depositional environment. The faunal resolution in the deeper zones is less precise, which makes subtle changes difficult to detect. Emergences in the MPE curves appear to be more gradual than submergences (Fig. 5), but the lack of detail in accretion rates prevents

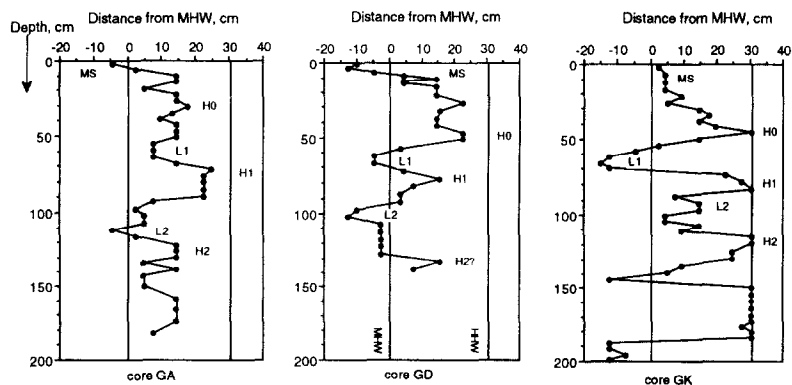


Fig. 5. Marsh paleoenvironment (MPE) curves for the three Guilford cores, based on foraminiferal zonations as defined in Fig. 2, and derived using faunal compositions as shown in Fig. 4. Submergence (*MS*, *L1*, *L2*) and emergence events (*H0*, *H1*, *H2*) as discussed in the text. Units are centimeters below (to left) or above (to right) MHW; MHW=mean high water level; HHW=highest high water level.

us from translating that information into a time frame.

3.3. Chemical data

Element profiles for sulfur (S), iron (Fe), copper (Cu) and zinc (Zn) are shown together with loss on ignition (LOI) data (Figs. 6 and 7). The Cu profiles mark the onset of anthropogenic metal pollution (A.D. 1877) most clearly, and we use this level as an isochronous surface through the whole marsh (Fig. 7). At this level we commonly see a strong increase in Zn concentrations, although Zn profiles show much more variation in the pre-pollution period than Cu profiles. The origin of the large Cu anomalies (116 and 168 ppm Cu) in cores GK and GA at about 1 m depth (i.e., about A.D. 1350) is a mystery; they are discussed together with further details of the pollution chemistry by Scholand et al. (in prep).

The acid-leachable S and Fe abundances in the cores show a good correlation (Fig. 6) and most samples plot in a band close to the pyrite stoichiometry (Fig. 8). High marsh environments have S abundances in excess of the pyrite stoichiometry, probably the result of the presence of S associated with organic matter. Samples with excess Fe with respect to the pyrite stoichiometry are clay-rich sediments where the amount of organic matter limited pyrite formation. Samples from core GK plot predominantly in the band between pyrite stoichiometry and the line pyrite+0.5% S, typical for high marsh peats. The samples from core GA plot for 60% in the low marsh zone (above the pyrite line), whereas the samples from core GD plot around the pyrite line and above.

S and Fe abundances show a good correlation with the GA “other species” curve, with S and Fe enrichments at high percentages of “other species”, except for the upper 10 cm (Fig. 9). The LOI curve shows a generally negative correlation with the faunal curve. The patterns of the GK core show an excellent agreement in the upper meter of the core and the bottom clay layer, but the section between 100 and 150 cm shows a fair amount of noise. The section between 150 and 190 cm had very few foraminifera, but the few preserved tests are not typical for a high-marsh environment

(Appendix 3). The S curve suggests an emergence event near 190 cm, in agreement with faunal data, but a gradual submergence from 180 cm upwards. This trend is shown by the Fe and S data, but the LOI data do not show evidence for a high marsh environment. Most likely, the fauna has been partially oxidized in the section between 150 and 180 cm depth, possibly also between 113–117 cm, 80–85 cm and 44–48 cm depth. The LOI curve of GK shows a very crude inverse correlation with the faunal curve. The chemical and faunal data from the GD site show more noise and an overall poor correlation.

3.4. Age determinations

Seventeen samples were selected for ^{14}C dating (Table 1). The undulations in the calibration curve may result in two age brackets for a single sample; in that case we report the complete range between the two bracketing ages. Several young intersections with the calibration curve were omitted based on the stratigraphic position of the sample (Table 1^c).

The paleommarsh-surface for each radiocarbon sample was determined from the growth position of the roots or rhizomes; it was taken in the middle of a slice for bulk samples (Table 1; Fig. 10). We present the data in age–depth graphs, in which “depth” is the depth of the paleommarsh surface below the modern marsh surface, which has an age of A.D. 1993. Foraminifera live on or close to the marsh surface, so that faunas have an age equal to that of their paleommarsh surface.

The age for sample GK6 is anomalously young, probably because this sample (bulk organic matter instead of roots picked by species) is contaminated by root-growth from above. We prefer to use the age of samples GK 4 and GK5, because these data were obtained from two different species of hand-picked roots of which the ages agree with each other. The onset of metal pollution in cores GA, GD and GK was found to occur respectively at approximately 20, 20 and 26 cm depth (Nydick, 1993), which represents the 1877 ± 15 A.D. age level (Green, 1988).

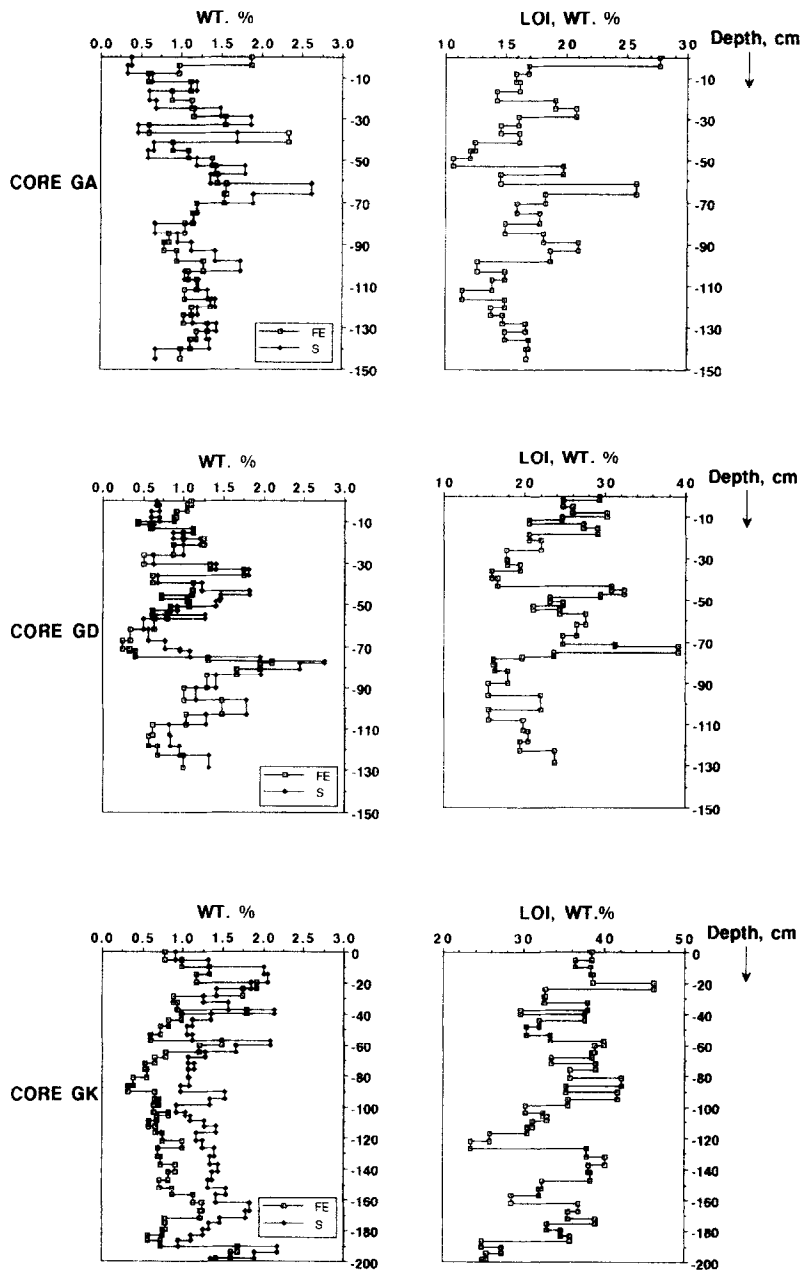


Fig. 6. Concentrations of Fe and S, and Loss on Ignition values (LOI).

4. Discussion

4.1. Accretion rates

Accretion rates in marshes vary strongly according to depositional environment, with high rates

in the low-marsh areas near the sea and near large creeks, and low rates in high-marsh zones far away from the sea and creeks (Pethick, 1981; French and Spencer, 1993; Allen, 1994). Our working model of marsh accretion can be summarized as follows: if the rate of RSLR increases, a given

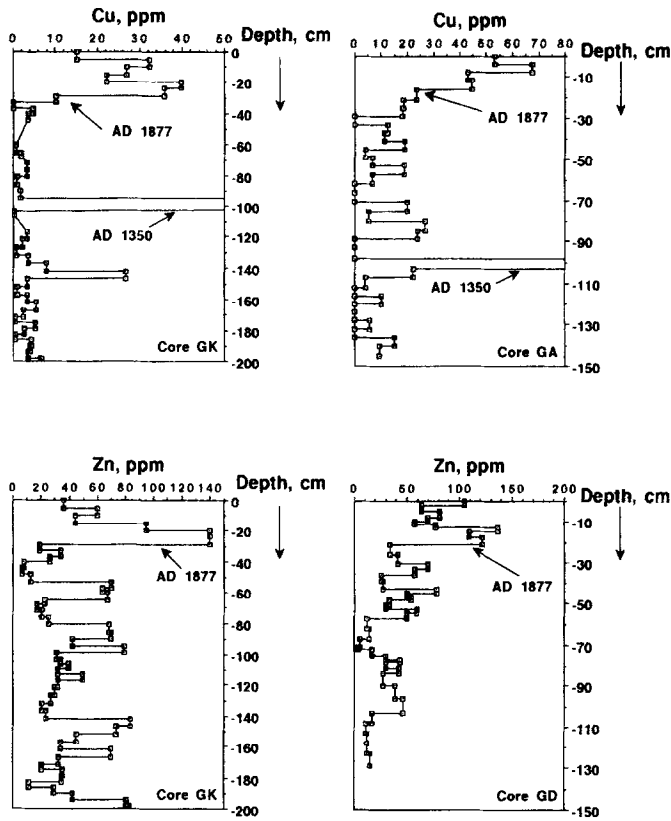


Fig. 7. Concentration of Cu in cores GK and GA, Zn in cores GK and GD. The onset of anthropogenic metal pollution is indicated as well as the mystery Cu peak around A.D. 1350.

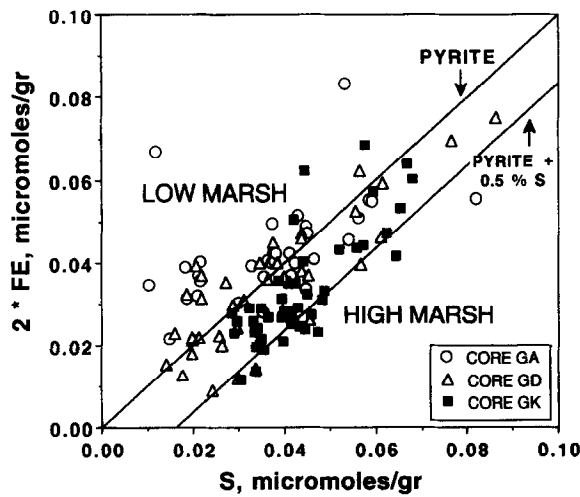


Fig. 8. Correlation of Fe and S contents in the three cores. The pyrite stoichiometry line (1:1) is shown as well as a lower boundary which represents sediments with pyrite and about 0.5% S associated with organic matter. High marsh environments plot to the right; clay-rich, low marsh environments to the left of the pyrite line.

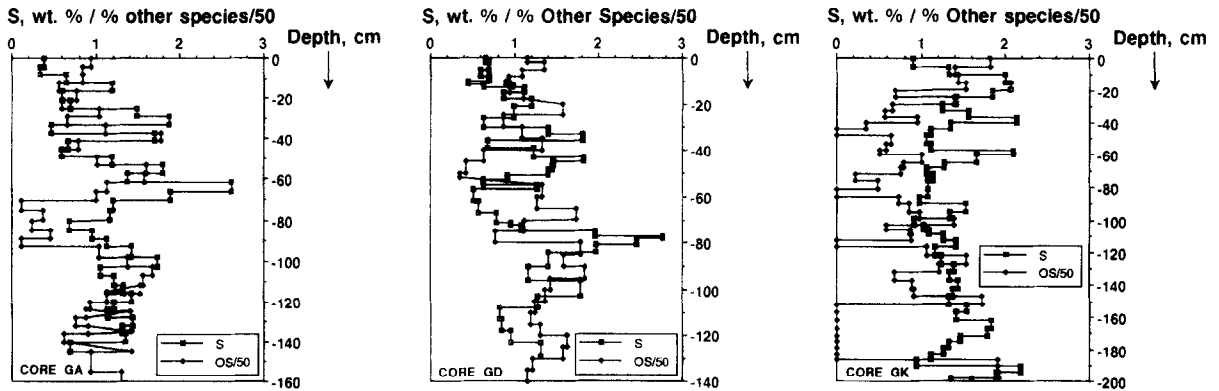


Fig. 9. Concentration of sulfur compared to the percentage of *other species* (i.e., 100% - % *T. macrescens*); the latter value is shown divided by 50 for easier comparison with the sulfur values.

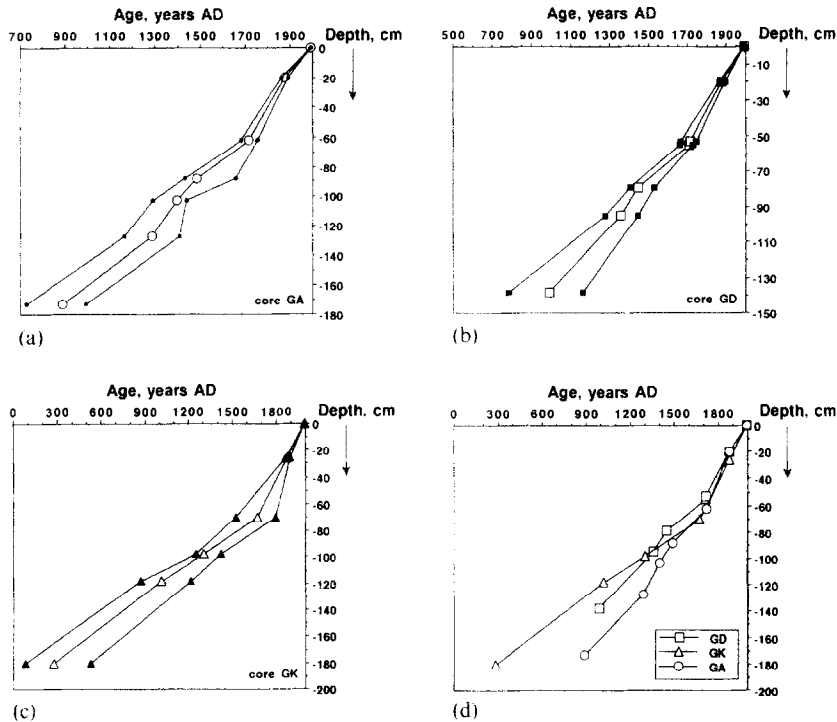


Fig. 10. Age-depth relationships for the Guilford cores with 2σ band of uncertainty (a: core GA; b: core GD; c: core GK; d: comparison of the age records for the three cores). The depth scale provides the depth of the paleommarsh surface below the modern marsh surface, and the slopes of the lines show the marsh-accretion rates.

marsh site will submerge and its depositional environment will thus shift to a lower marsh environment, where accretion rates are higher. Increased submergence of the marsh surface will cease once a depositional environment has been reached with

a rate of accretion equal to the rate of RSLR, the so-called equilibrium rate of accretion (Pethick, 1981; Allen, 1990a, 1992, 1994; Chmura et al., 1992). If the rate of RSLR slows down, the rate of marsh accretion at the site will outpace the rate

of RSLR and therefore the depositional environment will shift to higher marsh, where accretion rates are lower. Again, the environment keeps shifting until an equilibrium value has been reached. If a constant rate of RSLR persists for a long time, a large area of the marsh will acquire a similar depositional facies (mature marsh), with an accretion rate that is everywhere about equal to the rate of RSLR. This model explains broadly the existence of the wide flat plains of cordgrass that occupy the coastal areas along Long Island Sound. The environmental zonation and variations in accretion rate in the modern marsh suggest that the marshes are at the present time not mature.

The slopes of the three age-depth curves from the three cores in Guilford indicate variable marsh accretion rates (Fig. 10). The highest average rate occurs in core GA (1.6 mm/yr) which is closest to the sea, core GD has an intermediate rate (1.4 mm/yr), whereas core GK (most landward) had the lowest overall accretion rate (1.1 mm/yr). The values are comparable to accretion rates found in other marshes along Long Island Sound (e.g., Bloom and Stuiver, 1963; Harrison and Bloom, 1977; Van de Plassche et al., 1991; Patton and Horne, 1992; Varekamp et al., 1992).

We compared average accretion rates over the core interval corresponding to the last 1000 years to the average rate of mean high water rise (Table 2). At all core locations the rise in MHW over the last 1000 years outpaced the accretion rate, but not by very much. The lowest accretion and MHW rates occur at the most landward site, the highest rates at the most seaward site. The average rate of MHW derived from core F at the landward side of the Hammock River marshes (Varekamp et al., 1992; Table 2) is about 1.3 mm/yr for the last 1000 years, similar to that for core GK.

More seaward-located marsh sites experienced thus a higher rate of RSLR and had higher marsh accretion rates as well. Why would the rate of RSLR be higher at seaward marsh sites? The marsh sequence presumably has a wedge-shaped morphology going from sea to land (e.g., Redfield, 1972), and seaward-located marsh sites are underlain by a thicker sequence of marsh deposits, as confirmed by our field data (Nydick, 1993). A

Table 2

Rates of marsh accretion and MHW for the last 1000 years and for the last 200 years for cores from Guilford marsh (GA, GD, GK) and Clinton marsh (F). Δ rate (net-submergence rate) is the difference between the rate of MHW and rate of marsh accretion; the submergence index is their ratio

Rates, period covered	Core GA	Core GD	Core GK	Core F
Accretion rate, 1000 yrs	1.60	1.39	1.18	1.22
MHW rate, 1000 yrs	1.79	1.55	1.30	1.31
Δ rate, 1000 yrs	0.19	0.16	0.12	0.09
Submergence index, 1000 yrs	1.12	1.12	1.18	1.07
Accretion rate, 200 yrs	2.10	1.97	2.20	1.65
MHW rate, 200 yrs	2.85	3.26	3.09	2.67
Δ rate, 200 yrs	0.75	1.29	0.89	1.02
Submergence index, 200 yrs	1.36	1.65	1.40	1.62

thicker sequence will show more compaction than thin marsh veneers over glacial bedrock. Our ongoing study of peat density versus depth indicates that compaction and de-watering in the upper 2 m of marsh deposits is insignificant, but the deeper section de-waters and compacts (e.g., Harrison and Bloom, 1977), so that the overlying marsh section will “go along for the ride”. We therefore speculate that the seaward marsh sites have a larger subsidence component than the landward-sites, which is the sum of the regional crustal subsidence and a thickness-dependent compaction component of the deeper marsh sequence.

We currently can not correct for this effect, but the depositional and environmental development at each site depends on the combined rate of regional subsidence, overall compaction and sea-level rise, which is reflected in the type of deposit, accretion rate and average rate of RSLR. The net-submergence rates (rate of RSLR – accretion rate) over the last 1000 years vary from 0.12 to 0.19 mm/yr (Table 2), which implies a gradual deepening of the marsh surface of only 10–20 cm over a millennium. Obviously, on this time scale, the marshes keep up reasonably well with the rising tides.

The net-submergence rates over the last 200

years were much higher than the average over the last 1000 years in all cores (Table 2). All three sites show higher accretion rates over this interval, with about double the rates of RSLR of the average of the last 1000 years. These features can be conveniently expressed as the *submergence index*, the ratio of RSLR and accretion rate. This parameter had a value of 1.12–1.18 for the last 1000 years but a value of 1.4–1.7 over the last 200 years (Table 2). Obviously, all three sites are presently out of equilibrium, and with the current net-submergence the whole modern middle to high marsh may become a low marsh environment in a few centuries.

4.2. Relative sea-level rise curves

The MHW curves for the Guilford marshes were derived from the independent data sets for the three cores: for each core we made paleo-environmental reconstructions resulting in the MPE curves, which constrain the shape of MHW curves. The age data are also generated independently for each core; therefore each core provides an independently derived RSLR record. Our interpretations and comparisons between cores are thus independent of the altitudes of the coring sites.

The three records show reasonable overall agreement (Fig. 11), but each has its local excursions. Only in core GK do we have data from the period prior to A.D. 200, during which RSLR averaged 0.7 mm/yr. After the following sudden emergence RSL rose steadily at about 0.9 mm/yr until about A.D. 650, when a sudden submergence occurred. This was followed by more sluggish RSLR until A.D. 1050–1100, when there was a short period of submergence followed by sluggish RSLR (about 0.3 mm/yr) until about A.D. 1620. From A.D. 1600 to 1700 the rate of RSLR increased to 5.0 mm/yr. Between A.D. 1700 and 1800 there was another short period of more sluggish sea-level rise, followed by a rapid rate of about 2.9 mm/yr until the present day.

The rapid and strong apparent sea-level excursions recorded in core GK (rise and fall) around A.D. 200, 700 and 1650 may represent local effects related to changes in the course of the creek near the GK site (Fig. 11c), or to a period of increased

storminess (meteoric high waters). The sudden emergence around A.D. 200 followed by the occurrence of high-marsh environments for several centuries as indicated by the faunal parameters is puzzling, and not supported by the chemical data (too high S and Fe contents for highest marsh): this “emergence” may reflect either a local catastrophic event (e.g., an earthquake that raised the marsh surface about 40 cm), or establishment of a spit or bar during a major storm event that changed the tidal hydrology of the marsh. More data from this time interval are needed before we can reach reliable conclusions. The subsequent submergence around A.D. 650 was coeval with a similar sudden submergence in the Clinton marsh curve (Fig. 11d).

Core GA shows a moderate rate of RSLR from about A.D. 800 to 1300 (about 1 mm/yr average), with a short acceleration between A.D. 1000 and 1100. Another short acceleration occurred at about A.D. 1350, followed by a period of sluggish rise (about 0.4 mm/yr from A.D. 1400 to 1630). A much faster rate of RSLR began around A.D. 1630, which continued until the present day (about 2.8 mm/yr).

Core GD shows relatively rapid RSLR between A.D. 1050 and 1100, followed by steady RSLR from about A.D. 1100 to 1250. There was a short acceleration at about A.D. 1250 to 1300, but the net rise of RSLR between A.D. 1300 to 1700 was sluggish at about 0.7 mm/yr; from A.D. 1700 on, the rate of RSLR was about 3.1 mm/yr.

We can thus distinguish three periods in the Guilford records: (I) a period of steady RSLR from about A.D. 250 to 1100, at an average relative rate of about 0.9 mm/yr, possibly with an acceleration about A.D. 700. This period ended with a short interval of slightly higher rates of RSLR between A.D. 1000 and 1100; (II) a period of slow RSLR with small, non-marsh-wide excursions from about A.D. 1100 to 1600, with an average relative rate <0.5 mm/yr; and (III) the most-recent period of rapid sea-level rise, starting between A.D. 1600 and 1700, possibly with a short deceleration between A.D. 1700 and 1800, and lasting till modern times, with a relative rate in excess of 3 mm/yr.

These three periods are shown in a highly styl-

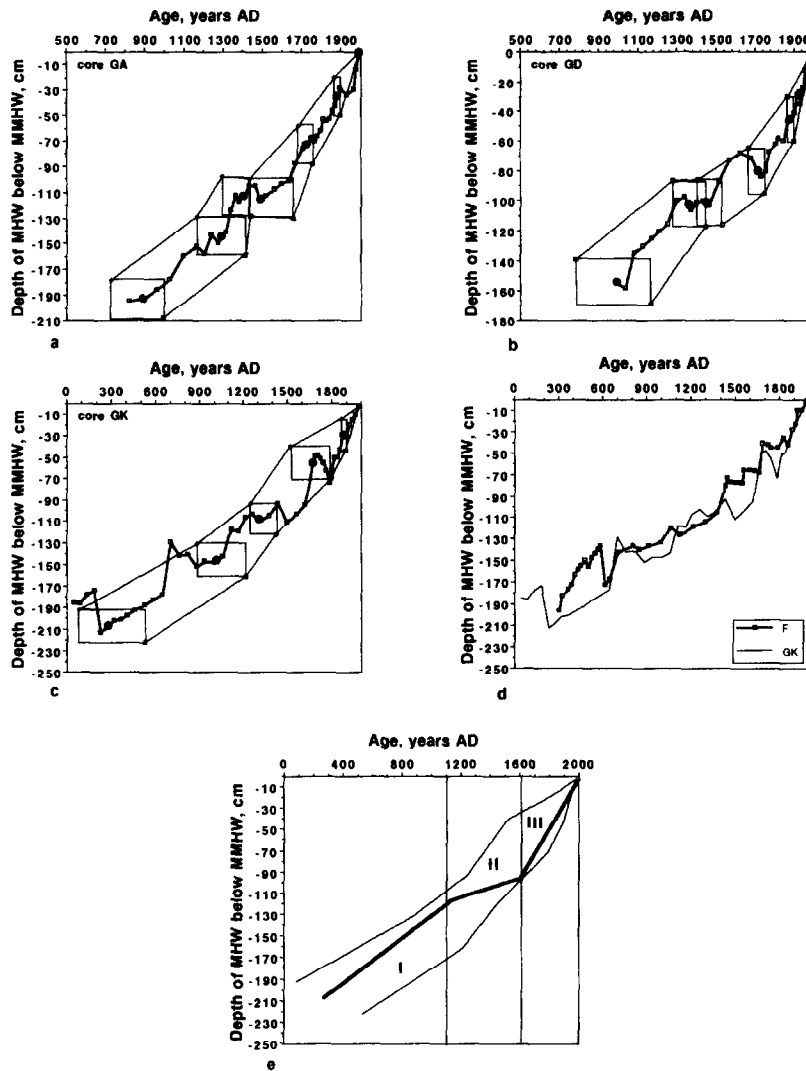


Fig. 11. Mean high water rise curves for the three Guilford cores (a, b, c), and for core F from the Hammock River marshes, Clinton, Connecticut (d; slightly modified after Varekamp et al., 1992). The heavily drawn lines are the MHW rise curves, constructed using the calibrated ages with interpolations in between, with the information from the MPE curves. The envelopes are drawn through the corners of the boxes which give the limits of the 2σ -age calibration and ± 15 cm precision in the estimates of paleo-MHW for each of the age marker points in the curves. Fig. 11e shows, in a schematic fashion, the three periods of RSLR that we distinguish, with an approximate overall error envelope. The shape of the RSLR curve is constrained by the MPE curves, and the uncertainty in the generalized curve is largely found in the fitting of a curve with that shape within the age–depth envelope.

ized fashion in Fig. 11e. One could possibly draw a straight RSLR line through the error envelope, which would discredit our conclusion that three periods existed with different rates of RSLR. The shape of the RSLR curve, however, is constrained by the information from the MPE curves, and only the duration, and beginning or end of the

three periods are related to the uncertainties within our age-model.

Our values of RSLR for the last 200 years (mean = 3.0 mm/yr) are slightly higher than the data from the New London, CT (2.1 mm/yr) and New York, NY (2.7 mm/yr) tide gauges over the last 130 years (Lyles et al., 1988). We explain this

difference of about 0.6 mm/yr as a result of additional subsidence of the marshes compared to the tide gauge sites as a result of marsh compaction as well as uncertainties in our age control.

4.3. Sea-level rise and climate change

The Guilford sea-level curves are local records potentially influenced by local tidal range fluctuations and the geomorphological development of the marsh. Comparison with the Clinton marshes (Connecticut; Varekamp et al., 1992) shows that in both marshes there were increased rates of RSLR from about A.D. 1600 to 1700 on, possibly with lower rates for a short period around A.D. 1700–1800 (Fig. 11). This increased rate of relative sea-level rise over the last few hundreds of years is a consistent feature of all our records (Varekamp and Thomas, work in progress).

The relation between small climate fluctuations and rates of SLR are tenuous: some stress that sea-level rise should be expected if global temperatures rise (e.g., Houghton et al., 1990, 1992; Wigley and Raper, 1992, 1993), whereas others argue that global warming should lead to lowered sea level, because higher temperatures at high latitudes will lead to enhanced precipitation, hence accretion of the polar ice sheets (e.g., Oerlemans, 1993). Others have concluded that there is essentially no correlation between climate and sea-level rise on the scale of minor climate fluctuations (e.g., Anderson, 1991; Anderson and Thomas, 1991). The fact that sea level has been rising at all over the last few thousand years is curious (e.g., Rampino, 1979; Allen and Rae, 1988; Fletcher et al., 1993b), because this period is not thought to have seen major net-warming (e.g., Overpeck, 1990; Webb, 1990).

Global temperature charts of the last 2000 years are rather uncertain (Bradley and Jones, 1992), but we can use the generalized summary in Houghton et al. (1990). The start of the first millennium was cool, but its middle period was warmer, with a significant cooling towards 800 A.D. The timing of the Little Climate Optimum is highly variable even within Europe, with a much later warming in Scandinavia (Grove, 1988). The Little Ice Age had very cold winters and hot summers, but a low average temperature (Lamb,

1977, 1984; Grove, 1988; Bradley and Jones, 1992). The timing and severity (or occurrence at all) of the Little Ice Age probably varied with location (Bradley and Jones, 1992; Lamb, 1977; Grove, 1988; Houghton et al., 1990).

We compared our RSLR data from about A.D. 700 on with the average temperature trends. The Little Climate Optimum is not characterized by an unusually high rate of RSLR, falling within our period I (Fig. 11e), although it may be reflected in the small pulse at A.D. 1050–1100 (Fig. 11a–c). Period II, between A.D. 1150 and 1600, may coincide with the early part of the Little Ice Age, and is characterized by a slow rate of RSLR. The period from A.D. 1650 to 1700 (start of period III) falls according to most authors still within the Little Ice Age, but clearly has an elevated rate of RSLR. The last 200 years are characterized by elevated rates of RSLR both in Guilford and in Clinton (Fig. 11).

5. Conclusions

Paleoenvironmental data from the Guilford marshes show that the modern coastal marshes with the large *S. patens* meadows fringed by *S. alterniflora* along creeks can not be seen as the “typical” marsh on time scales of centennia or more. Over a large part of the last 1500 years of their history, the Guilford marshes were more elevated (relative to mean sea level at that time) than they are today. Despite about two meters of RSLR over the last 1500 years, the marsh growth has been outpaced by RSLR only marginally, mainly during the last 350 years. We introduced the “submergence index” parameter, which quantifies the rate of net-submergence. The magnitude of this parameter may be used to constrain the significance of the increased rates of RSLR over the last few centennia in other locations. Over this period the rate of RSLR was faster than the accretion rates, so that the marshes have been submerging relative to MHW. If past trends continue, large areas that are presently middle marsh will submerge until they reach low-marsh elevations.

The Little Climate Optimum has been compared with the modern period of Global Warming (e.g.,

Warrick, 1993). Our data show a small acceleration in the rate of RSLR during the former period but the signals are close to the noise level and the imprecision in our time frame does not yet permit us to constrain the exact duration of such a pulse. During the early stages of the Little Ice Age RSLR was slow, but acceleration started in its middle part (as defined by most authors). The last 350 years have seen the fastest RSLR of the last 1500 years, as shown in the three cores from this study as well as the data from the Clinton marshes (Varekamp et al., 1992). The general onset of the higher rates of RSLR preceded the beginning of modern global warming, which started according to many authors late last century or early this century (Houghton et al., 1990).

Acknowledgements

This is a contribution to International Geological Correlation Programme (IGCP)

Project 274, Coastal Evolution in the Quaternary. Part of this paper results from an undergraduate senior honors thesis by Koren Nydick. Johan C. Varekamp and Ellen Thomas acknowledge funding from the Connecticut Sea Grant College Program through NOAA grant NA 90 AA-D-SG443, project R/OE-2, and NOAA grant GC91-301 through the Global Change Program of NOAA, NA26GP0020-02. We thank the following Wesleyan University students in the Department of Earth and Environmental Studies for their efforts in the field and in the laboratory: Stephen Scholand, John Pasch, Erika Gasper, and Maria Lara-Whelpley. We also thank Heather Swarz for her work during her NECUSE fellowship at Wesleyan University in the summer of 1992. Detailed reviews of the manuscript by Dr. D. Belknap and Dr. R. Oldale as well as by one of the editors of this special volume, Dr. M. Chrzastowski, were very helpful. We also acknowledge Dr. Orson van de Plassche for putting us onto the 'marsh trail'.

Appendix 1: Core GA

sample	depth	total	T. macrescens	T. inflata	T. comprimata	A. mexicana	H. manilaensis	M. fusca	P. ipohalina	thecamoebians	nr/gr
GA1	0.0- 4.0	315	166	74	52	14	1	8	0	0	54300
GA2	4.0- 8.0	112	65	26	11	6	0	4	0	3	3700
GA3	8.0- 12.0	99	57	22	20	0	0	0	0	0	335
GA4	12.0- 16.5	132	95	33	3	0	1	0	0	0	13000
GA5	16.5- 21.0	111	68	35	2	0	4	2	0	1	3400
GA6	21.0- 25.0	137	96	37	4	0	0	0	0	1	2518
GA7	25.0- 29.0	117	56	47	14	0	0	0	0	0	301
GA8	29.0- 33.0	89	60	14	13	0	0	0	0	2	405
GA9	33.0- 37.0	63	28	32	3	0	0	0	0	0	168
GA10	37.0- 41.0	124	14	63	47	0	0	0	0	0	335
GA11	41.0- 45.0	123	74	33	16	0	0	0	0	0	1046
GA12	45.0- 49.0	114	80	22	11	0	1	0	0	0	306
GA13	49.0- 53.0	114	56	3	55	0	0	0	0	0	699
GA14	53.0- 57.0	119	24	77	18	0	0	0	0	0	9900
GA15	57.0- 61.5	104	22	71	11	0	0	0	0	0	76
GA16	61.5- 66.0	85	37	21	27	0	0	0	0	1	240
GA17	66.0- 70.5	120	60	30	30	0	0	0	0	1	903
GA18	70.5- 75.0	128	121	6	0	1	0	0	0	1	1067
GA19	75.0- 78.0	108	88	19	1	0	0	0	0	0	7200
GA20	78.0- 83.0	111	98	12	0	1	0	0	0	1	1914
GA21	83.0- 88.0	100	77	23	0	0	0	0	0	1	699
GA22	88.0- 91.0	143	68	53	20	0	2	0	0	0	5743
GA23	91.0- 95.0	109	52	45	11	1	0	0	0	0	1817
GA24	95.0-100.0	119	37	56	20	6	0	0	0	5	2975
GA25	100.0-105.0	118	19	79	14	1	2	1	2	0	3050
GA26	105.0-110.0	150	33	104	11	1	0	1	0	0	11000
GA27	110.0-114.0	110	26	36	9	3	0	36	0	0	482
GA28	114.0-119.0	106	46	41	7	2	0	10	0	0	226
GA29	119.0-125.0	106	57	41	5	0	2	0	1	0	341
GA30	125.0-128.0	111	62	6	43	0	0	0	0	0	1781
GA31	128.0-132.0	114	71	13	30	0	0	0	0	0	6667
GA32	132.0-136.0	120	66	30	6	18	0	0	0	0	2659
GA33	136.0-140.0	109	75	16	18	0	0	0	0	1	2220
GA34	140.0-145.0	111	73	25	6	7	0	0	0	0	837
GA38	145.0-155.0	101	44	41	13	0	0	3	0	0	4810
GA39	155.0-162.0	132	39	83	10	0	0	0	0	0	10150
GA40	162.0-170.0	156	45	92	19	0	0	0	0	0	11143
GA41	170.0-178.0	115	61	32	21	1	0	0	0	0	19170
GA42	178.0-186.0	112	39	55	16	1	0	1	0	0	10182

Appendix 2: Core GD

sample	depth	total	T. macrescens	T. inflata	T. comprimata	A. mexicana	H. manilaensis	M. fusca	P. ipohalina	T. earlandi	calcareous	thecamoebians	nr/gr
GD1	0.0- 2.0	133	56	45	13	14	0	4	0	0	1	1	7000
GD2	2.0- 5.0	113	37	36	19	18	0	1	0	2	0	0	1883
GD3	5.0- 8.0	115	52	44	17	1	0	1	0	0	0	0	2880
GD4	8.0- 10.0	117	63	31	21	1	0	1	0	0	0	0	4680
GD5	10.0- 11.5	106	59	29	18	0	0	0	0	0	0	3	187
GD6	11.5- 13.0	108	53	27	25	3	0	0	0	0	0	1	6210
GD7	13.0- 15.0	129	68	30	25	6	0	0	0	0	0	0	6450
GD8	15.0- 18.0	120	54	43	22	0	1	0	0	0	0	0	5714
GDN1	20.0- 25.0	128	27	65	31	0	5	0	0	0	0	3	25600
GDN2	25.0- 30.0	172	97	51	24	0	0	0	0	0	0	1	8600
GDN3	30.0- 35.0	165	75	42	41	0	7	0	0	0	0	0	16500
GDN4	35.0- 40.0	101	34	21	43	0	3	0	0	0	0	0	3367
GDN5	40.0- 45.0	101	69	17	15	0	0	0	0	0	0	0	326
GDN6	45.0- 50.0	104	82	11	11	0	0	0	0	0	0	0	158
GDN7	50.0- 55.0	75	62	6	7	0	0	0	0	0	0	0	357
GDN8	55.0- 60.0	114	37	45	22	2	4	3	1	0	0	1	1310
GDN9	60.0- 65.0	123	45	18	34	0	0	14	12	0	0	22	1557
GDN10	65.0- 70.0	91	12	9	44	0	3	2	21	0	0	39	221
GDN11	70.0- 75.0	93	41	14	8	0	0	1	29	0	0	20	1141
GDN12	75.0- 80.0	115	71	17	24	0	0	0	3	0	0	1	2347
GDN13	80.0- 85.0	55	6	1	2	0	0	0	46	0	0	0	223
GDN14	85.0- 90.0	86	18	32	4	5	0	1	26	0	0	7	585
GDN15	90.0- 95.0	110	9	36	30	25	0	4	5	0	0	0	1146
GDN16	95.0-100.0	124	36	30	28	5	0	24	1	0	0	2	12400
GDN17	100.0-105.0	107	34	29	14	1	2	27	0	0	0	2	17833
GDN18	105.0-110.0	110	42	25	16	4	1	22	0	0	0	0	7333
GDN19	110.0-115.0	120	49	30	16	5	1	11	8	0	0	2	543
GDN20	115.0-120.0	103	36	35	16	8	1	5	1	0	0	1	2943
GDN21	120.0-125.0	80	15	12	12	5	0	4	32	0	0	3	254
GDN22	125.0-130.0	66	14	7	9	1	0	3	32	0	0	0	468
GDN23	130.0-135.0	117	46	21	14	0	0	0	46	0	0	11	696
GDN24	135.0-140.0	114	48	49	12	1	0	2	2	0	0	2	8143

Appendix 3: Core GK

sample	depth	total	T. macrescens	T. inflata	T. comprimata	A. mexicana	H. maniaensis	M. tusca	P. ipohalina	A. inepta	thecamoebians	nr/gr
GK1	0.0- 5.0	114	10	33	63	7	0	0	0	1	0	36774
GK2	5.0- 10.0	121	36	57	22	5	0	1	0	0	1	52609
GK3	10.0- 15.0	118	33	24	59	2	0	0	0	0	0	29500
GK4	15.0- 20.0	114	27	48	32	1	0	5	1	0	0	21509
GK5	20.0- 24.0	101	66	14	21	0	0	0	0	0	0	38846
GK6	24.0- 29.0	114	35	76	2	1	0	0	0	0	0	18689
GK7	29.0- 33.0	128	86	28	14	0	0	0	0	0	0	51200
GK8	33.0- 37.0	102	73	25	3	0	0	1	0	0	0	25500
GK9	37.0- 40.0	160	84	49	20	0	6	1	0	0	0	26700
GK10	40.0- 44.0	108	89	4	12	0	0	3	0	0	0	36000
GK11	44.0- 48.0	3	1	2	0	0	0	0	0	0	0	140
GK12	48.0- 53.0	102	69	11	21	1	0	0	0	0	0	34000
GK13	53.0- 57.0	119	84	3	18	6	0	7	0	1	0	42500
GK14	57.0- 60.0	144	107	9	17	0	1	10	0	0	0	102857
GK15	60.0- 65.0	117	58	24	25	3	0	5	0	2	0	55714
GK16	65.0- 68.0	235	142	39	37	5	0	0	12	1	0	40517
GK17	68.0- 72.0	114	71	1	37	1	0	0	0	4	0	25300
GK18	72.0- 76.0	107	95	6	6	0	0	0	0	0	1	10000
GK19	76.0- 81.0	25	19	2	4	0	0	0	0	0	1	1920
GK20	81.0- 86.0	5	1	0	0	0	0	0	4	0	6	228
GK21	86.0- 90.0	110	70	15	16	1	5	2	1	0	7	3550
GK22	90.0-95.0	35	20	8	6	0	0	0	1	0	0	5830
GK23	95.0- 99.0	104	53	19	21	0	9	0	1	1	0	34700
GK24	99.0-103.0	213	65	53	57	3	35	0	0	0	2	38036
GK25	103.0-106.0	160	113	14	23	2	6	1	1	0	0	40000
GK26	106.0-109.0	67	38	8	20	0	0	0	0	1	0	1017
GK27	109.0-113.0	109	61	24	17	3	3	0	0	1	0	2633
GK28	113.0-117.0	17	6	1	7	0	1	2	0	0	1	444
GK29	117.0-122.0	28	13	6	4	1	2	0	0	2	1	952
GK30	122.0-127.0	30	7	6	13	0	3	0	1	0	0	641
GK31	127.0-132.0	28	11	6	9	0	0	0	0	2	2	915
GK32	132.0-137.0	103	68	14	13	1	1	1	2	3	2	1932
GK33	137.0-142.0	121	67	13	32	0	3	0	2	4	0	3954
GK34	142.0-147.0	58	32	7	12	0	0	3	0	5	0	1621
GK35	147.0-152.0	42	6	2	34	0	1	0	1	0	1	1080
GK36	152.0-157.0	15	5	3	4	2	0	0	1	0	2	949
GK37	157.0-162.0	10	6	0	4	0	0	0	0	0	0	172
GK38	162.0-167.0	20	10	3	7	0	0	0	0	0	1	447
GK39	167.0-172.0	15	11	3	1	0	0	0	0	0	0	528
GK40	172.0-175.0	6	3	1	0	0	0	0	1	0	0	195
GK41	175.0-179.0	29	17	3	3	0	0	0	4	2	4	564
GK42	179.0-183.0	8	2	0	0	0	0	0	6	0	9	311
GK43	183.0-186.0	18	0	2	1	0	0	0	15	0	10	1017
GK44	186.0-190.0	105	5	37	20	43	0	0	0	0	3	4907
GK45	190.0-194.0	187	9	46	32	100	0	0	0	0	1	34000
GK46	194.0-198.0	103	4	9	63	24	1	1	1	0	0	17167
GK47	198.0-201.0	199	40	66	47	32	8	6	0	0	0	66300

References

- Allen, J.R.L., 1987. Toward a quantitative chemostratigraphic model for sediments of late Flandrian age in the Severn estuary. *Sediment. Geol.*, 53: 73–100.
- Allen, J.R.L., 1990a. Constraints on measurement of sea-level movements from salt-marsh accretion rates. *J. Geol. Soc., London*, 145: 5–7.
- Allen, J.R.L., 1990b. The formation of coastal peat marshes under an upward tendency of relative sea-level. *J. Geol. Soc., London*, 147: 743–745.
- Allen, J.R.L., 1990c. Salt-marsh growth and stratification; a numerical model with special reference to the Severn estuary, southwest Britain. *Mar. Geol.*, 95: 77–96.
- Allen, J.R.L., 1991. Salt-marsh accretion and sea-level movement in the inner Severn estuary, southwest Britain: the archaeological and historical connection. *J. Geol. Soc., London*, 148: 485–494.
- Allen, J.R.L., 1992. Tidally influenced marshes in the Severn Estuary, southwest Britain. In: J.R.L. Allen and K. Pye (Editors), *Saltmarshes: Morphodynamics, Conservation and Engineering Significance*. Cambridge Univ. Press, Cambridge, UK, pp. 123–147.
- Allen, J.R.L., 1994. A continuity-based sedimentological model or temperate-zone tidal salt marshes. *J. Geol. Soc., London*, 151: 41–49.
- Allen, J.R.L. and Rae, J.E., 1988. Vertical salt-marsh accretion since the Roman period in the Severn estuary, southwest Britain. *Mar. Geol.*, 83: 225–235.
- Anderson, J.B., 1991. Marine records of late Quaternary glacial-interglacial fluctuations in the Ross Sea and evidence for rapid, episodic sea level change due to marine ice sheet collapse. In: R.A. Bindschadler (Editor), *West Antarctic Ice Sheet Initiative*. NASA Conf. Publ., 3115(2): 87–110.
- Anderson, J.B. and Thomas, F., 1991. Marine ice-sheet decoupling as a mechanism for rapid, episodic sea-level change: the record of such events and their influence on sedimentation. *Sediment. Geol.*, 70: 87–104.
- Belknap, D.F. and Kraft, J. C., 1977. Holocene relative sea-level changes and coastal stratigraphic units on the northwest flank of the Baltimore Canyon Trough geosyncline. *J. Sediment. Petrol.*, 47: 610–629.
- Berner, R.A., 1984. Sedimentary pyrite formation: an update. *Geochim. Cosmochim. Acta*, 48: 605–616.
- Berner, R.A., 1985. Sulphate reduction, organic matter decomposition and pyrite formation. *Philos. Trans. R. Soc., London*, A315: 25–38.
- Bertness, M.D., 1992. The ecology of a New England salt marsh. *Am. Sci.*, 80: 260–268.
- Bloom, A.L., 1964. Peat accumulation and compaction in a Connecticut coastal marsh. *J. Sediment. Petrol.*, 34: 599–603.
- Bloom, A.L. and Stuiver, M., 1963. Submergence of the Connecticut coast. *Science*, 139: 332–334.
- Bradley, R.S. and Jones, P.D. (Editors), 1992. *Climate since AD 1500*. Chapman and Hall, New York, 678 pp.
- Canfield, D.E., 1989. Reactive iron in marine sediments. *Geochim. Cosmochim. Acta*, 53: 619–632.
- Chmura, G., Costanza, R. and Kesters, E.C., 1992. Modelling coastal marsh stability in response to sea level rise: a case study in coastal Louisiana, USA. *Ecol. Model.*, 64: 47–64.
- Douglas, B.C., 1991. Global sea level rise. *J. Geophys. Res.*, 96: 6981–6992.
- Douglas, B.C., 1992. Global sea level rise acceleration. *J. Geophys. Res.*, 97: 12,699–12,706.
- Ember, L.M., Williams, D.F. and Morris, J.T., 1987. Processes that influence carbon isotope variations in salt marsh sediments. *Mar. Ecol. Progr. Ser.*, 36: 33–42.
- Fletcher, C.H., III, Pizzuto, J.E., Suku, J. and Van Pelt, J.E., 1993a. Sea-level rise acceleration and the drowning of the Delaware bay coast at 1.8 ka. *Geology*, 21: 121–124.
- Fletcher, C.H., III, Van Pelt, J.E., Brush, G.S. and Sherman, J., 1993b. High-resolution stratigraphic framework, Holocene sea-level and climate history, and evolution of a tidal wetland. *Palaeogeogr., Palaeoclimatol., Palaeoecol.*, 102: 177–213.
- French, J. Spencer, T. and Stoddart, D., 1990. Backbarrier salt marshes of the north Norfolk coast: geomorphic development and response to rising sea levels. Discussion Pap. Conservation, Univ. College London, London, UK, 34, 35 pp.
- French, J.R. and Spencer, T., 1993. Dynamics of sedimentation in a tide-dominated backbarrier salt marsh, Norfolk, UK. *Mar. Geol.*, 110: 315–331.
- Gayes, P.T., Scott, D.B., Collins, E.S. and Nelson, D.D., 1992. A late Holocene sea-level fluctuation in South Carolina. *SEPM Spec. Publ.*, 48: 155–160.
- Giblin, A., 1988. Pyrite formation in marshes during early diagenesis. *Geomicrobiol. J.*, 6: 77–97.
- Gornitz, V., 1992. Mean sea level changes in the recent past. In: R.A. Warrick, E.M. Barrow and T.M.L. Wigley (Editors), *Climate and Sea Level Change: Observations, Projections, and Implications*. Cambridge Univ. Press, Cambridge, UK, pp. 25–44.
- Groeger, M. and Plag, H.-P., 1993. Estimations of a global sea-level trend: limitations from the structure of the PSMSL global sea level data set. *Global Planet. Change*, 8: 161–179.
- Green, W.C., 1988. Utilizing Pb-210 to determine rates of accretion, trace metal fluxes and accumulations in a Guilford, CT salt marsh. Undergraduate Thesis, Yale Univ.
- Grove, J.M., 1988. *The Little Ice Age*. Methuen, London, 498 pp.
- Harrison, E.Z. and Bloom, A.L., 1977. Sedimentation rates on tidal salt marshes in Connecticut. *J. Sediment. Petrol.*, 47: 1484–1490.
- Houghton, J.T., Jenkins, G.J. and Ephraums, J.J. (Editors), 1990. *Climate Change: the IPCC Sci. Assessment*. Cambridge Univ. Press, Cambridge, UK, 365 pp.
- Houghton, J.T., Callander, B.A. and Varney, S.K. (Editors), 1992. *Climate Change 1992. Supplementary Rep. IPCC Sci. Assessment*. Cambridge Univ. Press, Cambridge, UK, 200 pp.
- Lamb, H.H., 1977. *Climate: Present, Past and Future, 2: Climatic History and the Future*. Methuen, London, 835 pp.
- Lamb, H.H., 1984. *Climate in the last 1000 years: natural*

- climatic fluctuations and change. In: H. Flohn and R. Fantechi, (Editors), *The Climate of Europe: Past, Present and Future*. Riedel, Dordrecht, pp. 25–64.
- Lambeck, K., 1990. Late Pleistocene, Holocene and present sea-levels: constraints on future change. *Global Planet. Change (Palaeogeogr., Palaeoclimatol., Palaeoecol.)*, 89: 205–217.
- Lyles L.D., Hickman L.E., Jr. and Debaugh H.A. Jr., 1988. Sea level variations for the United States, 1855–1986. NOAA Doc., US Dep. Comm., Rockville, Md.
- McCaffrey R.J. and Thomson J., 1980. A record of the accumulation of sediment and trace metals in a Connecticut salt marsh. In: B. Saltzman (Editor), *Estuarine Physics and Chemistry: Studies in Long Island Sound*. Adv. Geophys., 22: 165–236.
- Mörner, N.-A., 1993. Global change: the last millennia. *Global Planet. Change*, 8: 211–217.
- National Ocean Service, 1992. *Tide Tables 1992*. NOAA, U.S. Gov. Print. Off., Washington, DC.
- Niering, W.A., Warren, R.S. and Weymouth, C., 1977. Our dynamic tidal marshes: vegetation changes as revealed by peat analysis. (*Conn. Arboretum Bull.*, 22.) New London, CT, 12 pp.
- Nixon, S.W., 1982. The ecology of New England high salt marshes: a community profile. U.S. Fish Wildlife Serv., Off. Biol. Serv., Washington, DC., FWS/OBS-81-55, 70 pp.
- Nydick, K., 1993. Guilford salt marsh evolution and relative sea level rise. Undergraduate Honors Thesis, Wesleyan Univ., Middletown, CT.
- Oerlemans, J., 1993. Possible changes in the mass balance of the Greenland and Antarctic ice sheets and their effects on sea level. In: R.A. Warrick, E.M. Barrow and T.M.L. Wigley (Editors), *Climate and Sea Level Change: Observations, Projections, and Implications*. Cambridge Univ. Press, pp. 144–161.
- Orson, R.A., Warren, R.S. and Niering, W.A., 1987. Development of a tidal marsh in a New England river valley. *Estuaries*, 10: 20–27.
- Overpeck, J.T., 1990. Century- to Millennium scale climatic variability during the late Quaternary. In: R.S. Bradley (Editor), *Global Changes of the Past*. UCAR/Office for Interdisc. Earth Stud., Boulder, CO, pp. 139–173.
- Patton, P.C. and Horne, G.H., 1992. Response of the Connecticut River estuary to late Holocene sea level rise. *Geomorphology*, 5: 391–417.
- Peltier, W.R. and Tushingham, A.M., 1991. Influence of glacial isostatic adjustment on tide-gauge measurements of secular sea level change. *J. Geophys. Res.*, 96(B4): 6779–6796.
- Pethick, J.S., 1981. Long-term accretion rates on tidal salt marshes. *J. Sediment. Petrol.*, 51: 571–577.
- Rampino, M.R., 1979. Holocene submergence of southern Long Island. *Nature*, 280: 132–134.
- Redfield, A.C., 1967. Postglacial change in sea level in the western North Atlantic Ocean. *Science*, 157: 687–692.
- Redfield, A.C., 1972. Development of a New England salt marsh. *Ecol. Monogr.*, 42: 201–236.
- Redfield, A.C. and Rubin, M., 1962. The age of salt marsh peat and its relation to recent changes in sea level at Barnstable, Mass. *Proc. Natl. Acad. Sci.*, 48: 1728–1735.
- Roemmich, D., 1992. Ocean Warming and Sea Level Rise along the southwest US. *Coastal Sci.*, 257: 373–375.
- Scott, D.K. and Leckie, M.R.M., 1990. Foraminiferal zonation of Great Sippewissett Salt Marsh (Falmouth, Massachusetts), *J. Foraminiferal Res.*, 20: 248–266.
- Scott, D.B. and Medioli, F.S., 1978. Vertical zonation of marsh foraminifera as accurate indicators of former sea-levels. *Nature*, 272: 528–531.
- Scott, D.B. and Medioli, F.S., 1980. Quantitative studies of marsh foraminiferal distributions in Nova Scotia: implications for sea level studies. *Cushman Found. Foraminiferal Res. Spec. Publ.*, 17, 58 pp.
- Scott, D.B. and Medioli, F.S., 1986. Foraminifera as sea-level indicators. In: O. van de Plassche (Editor), *Sea-level Research: a Manual for the Collection and Evaluation of Data*. Geo Books, Norwich, UK, pp. 435–455.
- Scott, D.B., Medioli, F.S. and Miller, A.A.L., 1986. Holocene sea levels, paleoceanography, and late glacial ice configuration near the Northumberland Strait, Maritime Provinces. *Can. J. Earth Sci.*, 24: 668–675.
- Scott, D.B., Boyd, R. and Medioli, F.S., 1987. Relative sea-level changes in Atlantic Canada: observed level and sedimentological changes vs. theoretical models. *SEPM Spec. Publ.*, 41: 87–96.
- Scott, D.B., Suter, J.R. and Kosters, L., 1991. Marsh Foraminifera and arcellaceans of the lower Mississippi Delta: controls on spatial distributions. *Micropaleontology*, 37: 373–392.
- Shennan, I., 1986a. Flandrian sea-level changes in the Fenland. I. The geographical setting and evidence of sea level changes. *J. Quat. Science*, 1: 119–154.
- Shennan, I., 1986b. Flandrian sea level changes in the Fenland. II. Tendencies of sea-level movement, altitudinal changes, and local and regional factors. *J. Quat. Science*, 1: 155–180.
- Stuiver, M. and Pearson, G.W., 1993. High precision bidecadal calibration of the radiocarbon time scale, AD 1950–500 BC and 2500–6000 BC. *Radiocarbon*, 35: 1–23.
- Thomas, E. and Varekamp, J.C., 1991. Paleo-environmental analyses of marsh sequences (Clinton, CT): evidence for punctuated rise in relative sea level during the latest Holocene. *J. Coastal Res., Spec. Issue*, 11: 125–158.
- Thomson, J., Turekian, K.K. and McCaffrey, J.M., 1975. The accumulation of metals in and release from sediments of Long Island Sound. In: L.E. Cronin (Editor), *Estuarine Research, I: Chemistry, Biology and the Estuarine System*. Academic Press, New York, pp. 28–44.
- Tooley, M.J., 1982. Sea-level changes in Northern England. *Proc. Geol. Assoc.*, 93: 43–51.
- Tooley, M.J., 1993. Long term changes in eustatic sea level. In: R.A. Warrick, E.M. Barrow and T.M.L. Wigley (Editors), *Climate and Sea Level Change: Observations, Projections, and Implications*. Cambridge Univ. Press, pp. 81–110.
- Turekian, K.K., Cochran, J.K., Benninger, L.K. and Aller, R.C., 1980. The sources and sinks of nuclides in Long Island

- Sound. In: B. Saltzman (Editor), *Estuarine Physics and Chemistry: Studies in Long Island Sound*. Adv. Geophys., 22: 129–164.
- Van de Plassche, O., 1991. Late Holocene sea level fluctuations on the shore of Connecticut inferred from transgressive and regressive overlap boundaries in salt marsh deposits. *J. Coastal Res., Spec. Issue*, 11: 159–180.
- Van de Plassche, O., Mook, W.G. and Bloom, A.L., 1989. Submergence of coastal Connecticut 6000–3000 (^{14}C years). *Mar. Geol.*, 86: 349–354.
- Varekamp J.C., 1991. Trace element geochemistry and pollution history of mud flats and marsh sediments from the Connecticut River estuary. *J. Coastal Res., Spec. Issue*, 11: 105–124.
- Varekamp, J.C., Thomas, E. and Van de Plassche, O., 1992. Relative sea-level rise and climate change over the last 1500 years (Clinton, CT, USA). *Terra Nova*, 4: 293–304.
- Warrick, R.A., 1993. Climate and sea level change: a synthesis. In: R.A. Warrick, E.M. Barrow and T.M.L. Wigley (Editors), *Climate and Sea Level Change: Observations, Projections, and Implications*. Cambridge Univ. Press, pp. 2–24.
- Webb, T., III, 1990. The spectrum of climatic variability: current estimates and the need for global and regional time series. In: R.S. Bradley (Editor), *Global Changes of the Past*. UCAR/Office for Interdisc. Earth Stud., Boulder, CO, pp. 61–81.
- Wigley, T.M.L., 1990. Climate variability on the 10–100 year time scale: observations and possible causes. In: R.S. Bradley (Editor), *Global Changes of the Past*. UCAR/Office for Interdisc. Earth Stud. Boulder, CO, pp. 83–101.
- Wigley, T.M.L. and Raper, S.C.B., 1992. Implications for climate and sea level of revised IPCC emissions scenarios. *Nature*, 357: 293–300.
- Wigley, T.M.L. and Raper, S.C.B., 1993. Global mean sea level projections under the 1992 IPCC emissions scenarios. In: R.A. Warrick, E.M. Barrow and T.M.L. Wigley (Editors), *Climate and Sea Level Change: Observations, Projections, and Implications*. Cambridge Univ. Press, pp. 401–404.
- Woodworth, P.L., 1993. Sea level changes. In: R.A. Warrick, E.M. Barrow and T.M.L. Wigley (Editors), *Climate and Sea Level Change: Observations, Projections, and Implications*. Cambridge Univ. Press, pp. 379–391.